Supporting Information

Au-doped intermetallic Pd_3Pb wavy nanowires as highly efficient electrocatalysts toward oxygen reduction reaction

Sai Luo,[a] Dazhe Xu,[b] Junjie Li,[a] Yuxuan Huang,[a] Lei Li,[a] Xiao Li,[a] Xingqiao Wu,[a] Mingxi Gao,[a] Deren Yang[a] and Hui Zhang[a]*

[a]State Key Laboratory of Silicon Materials, School of Materials Science & Engineering, Zhejiang University, Hangzhou, Zhejiang 310027, People's Republic of China.

[b]Center for High Pressure Science and Technology Advanced Research, Pudong, Shanghai, 201203, People's Republic of China.

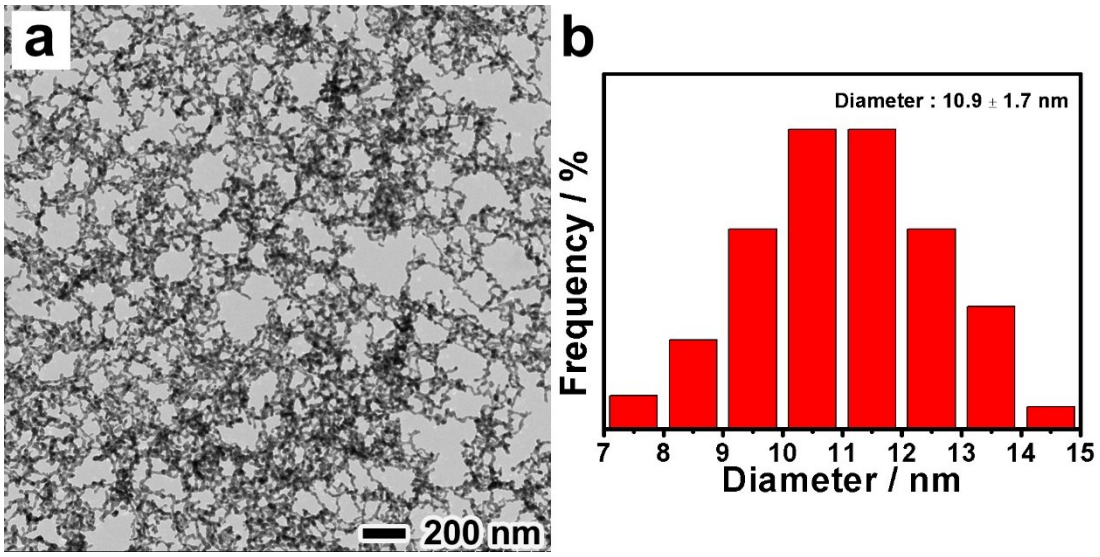

Figure S1. (a) Representative TEM image of the 2% Au-Pd_3Pb WNWs at low magnification and (b) the corresponding diameter distribution.

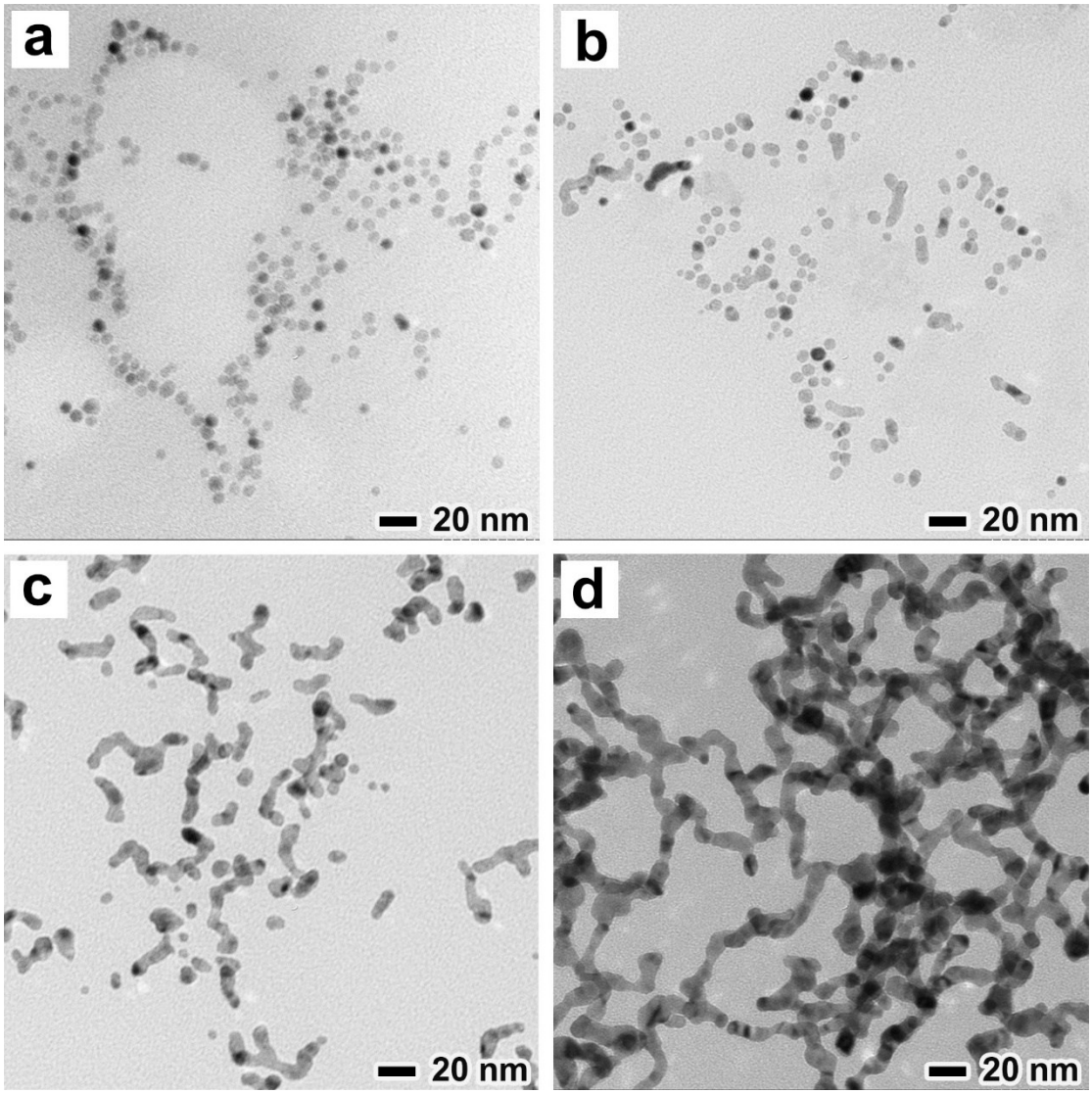

Figure S2. TEM images of the products prepared using the standard procedure, except for different reaction times: (a) 1, (b) 2, (c) 5, and (d) 10 min.

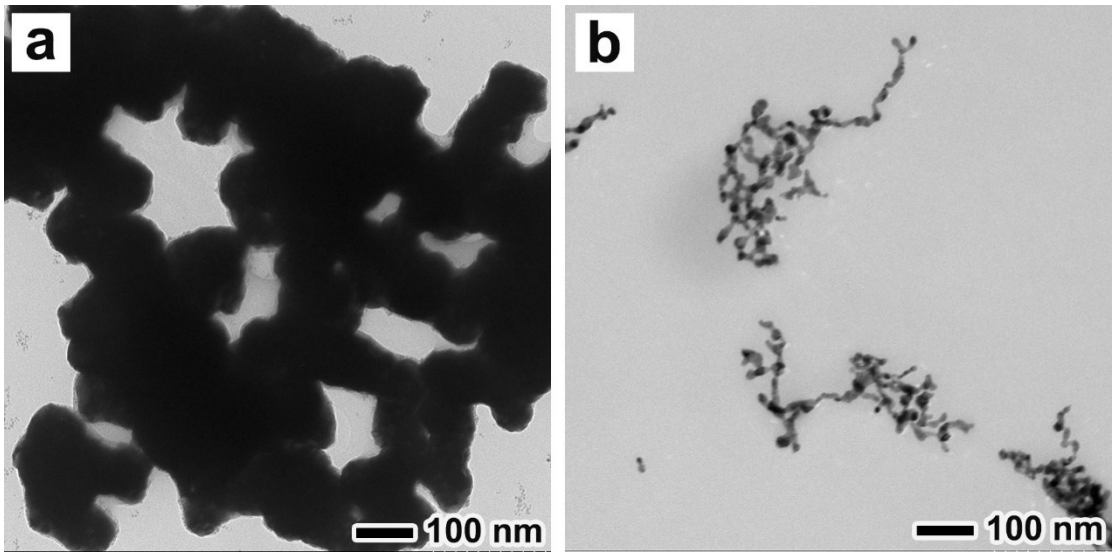

Figure S3. Representative TEM image of the products prepared by using the starndard procedure for the synthesis of the 2% Au-Pd_3Pb WNWs in the absence of (a) PVP and (b) AA.

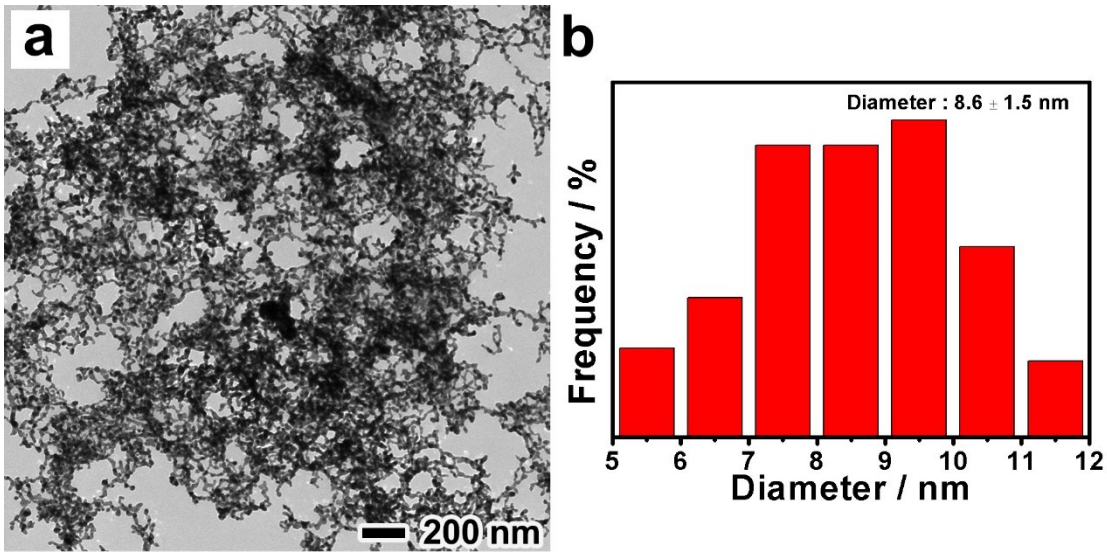

Figure S4. (a) Representative TEM image of the Pd_3Pb WNWs at low magnification and (b) the corresponding diameter distribution.

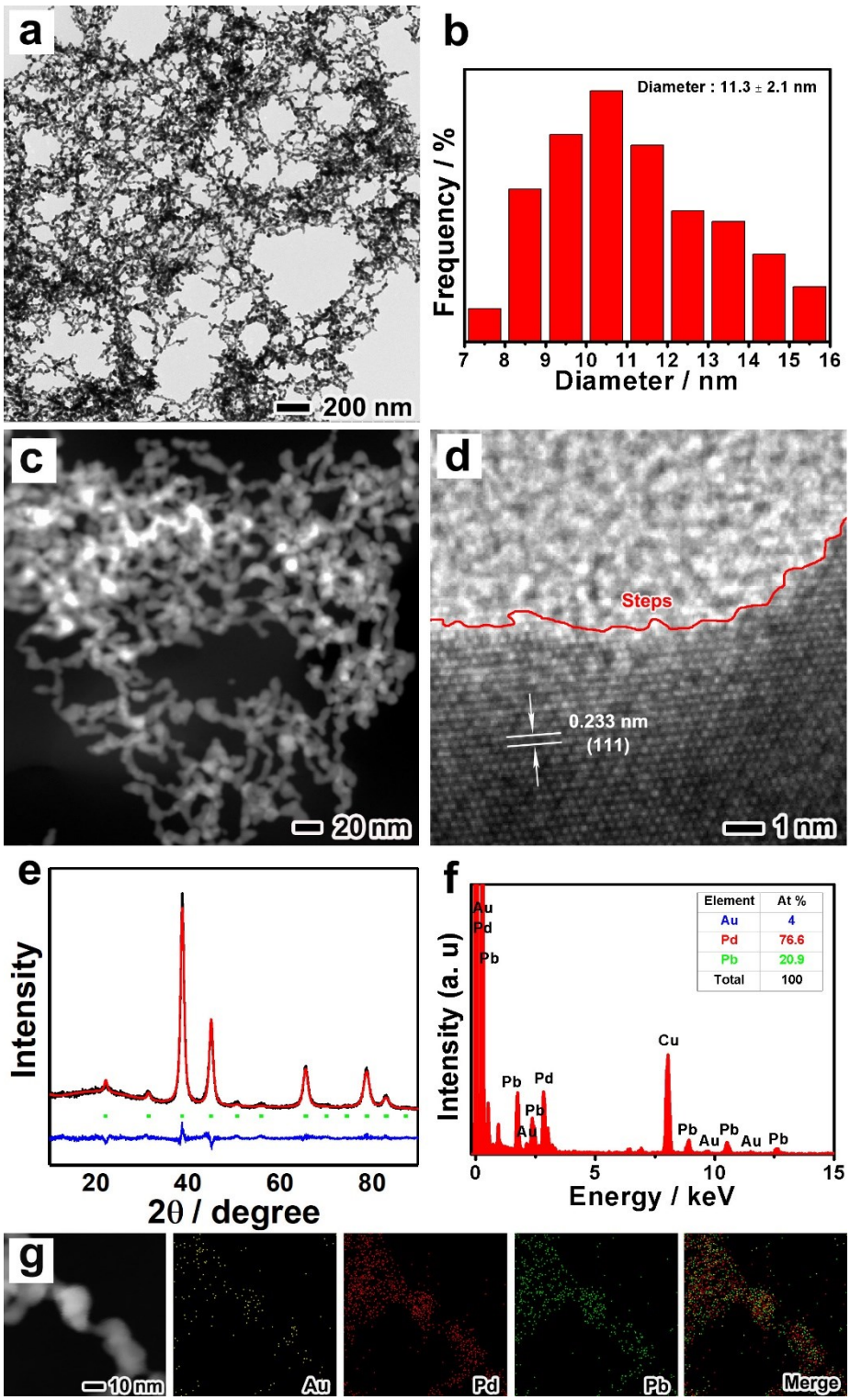

Figure S5. (a) TEM image, (b) the corresponding diameter distribution, (c) HADDF-STEM image, (d) HRTEM image, (e) Rietveld refinements of PXRD pattern, (Black line represents experimental data, red line represents simulated curve, blue curve is the difference and green bars represent index of Pd_3Pb), (f) EDX spectrum, and (g) EDX mapping images of the 4% Au-Pd_3Pb WNWs.

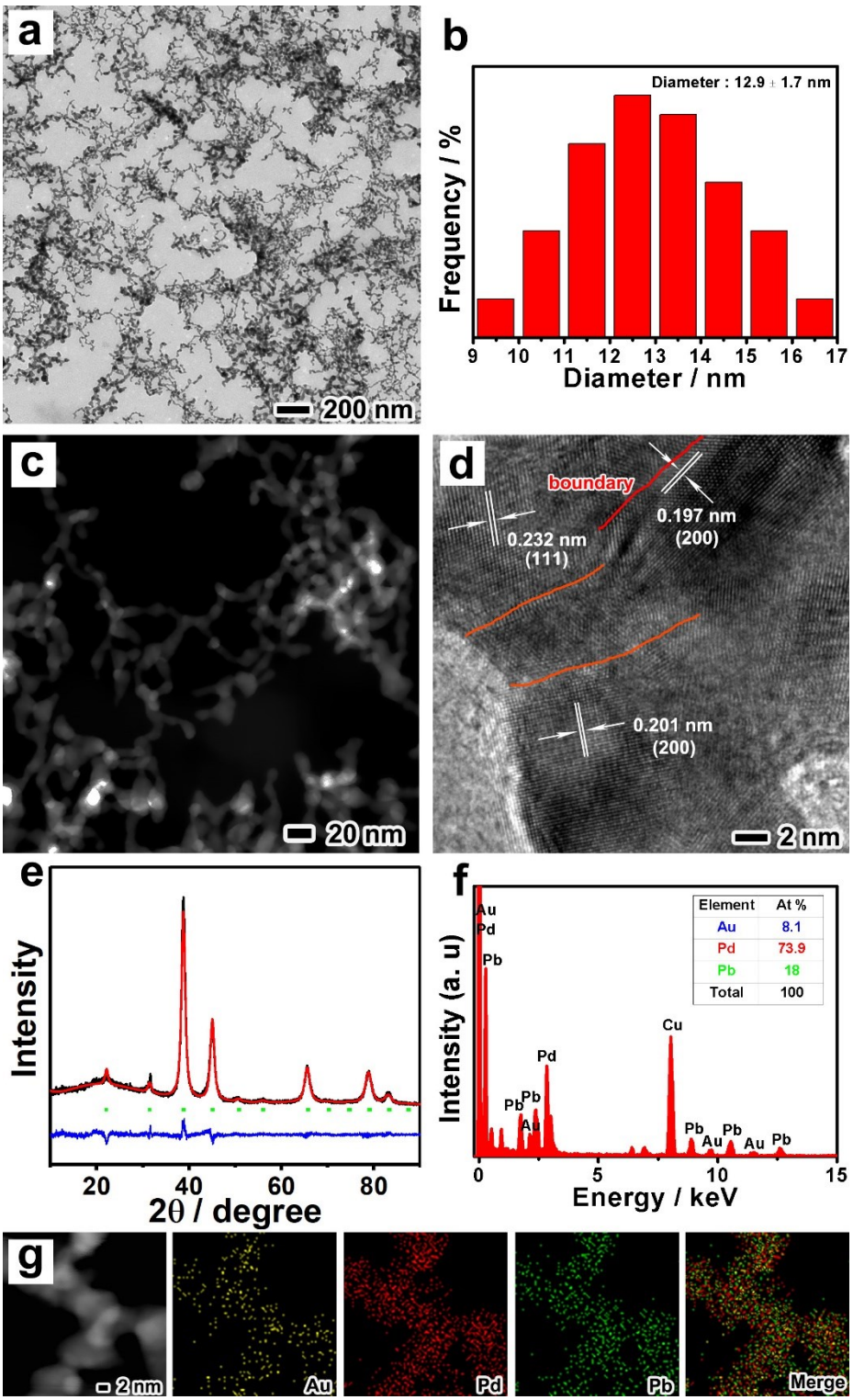

Figure S6. (a) TEM image, (b) the corresponding diameter distribution, (c) HADDF-STEM image, (d) HRTEM image, (e) Rietveld refinements of PXRD pattern, (Black line represents experimental data, red line represents simulated curve, blue curve is the difference and green bars represent index of Pd_3Pb), (f) EDX spectrum, and (g) EDX mapping images of the 8% Au-Pd_3Pb WNWs.

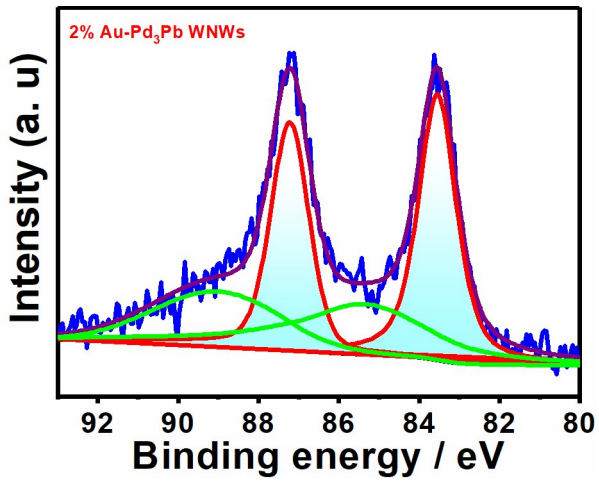

Figure S7. The XPS spectra of the 2% Au-Pd_3Pb WNWs for Au 4f orbital.

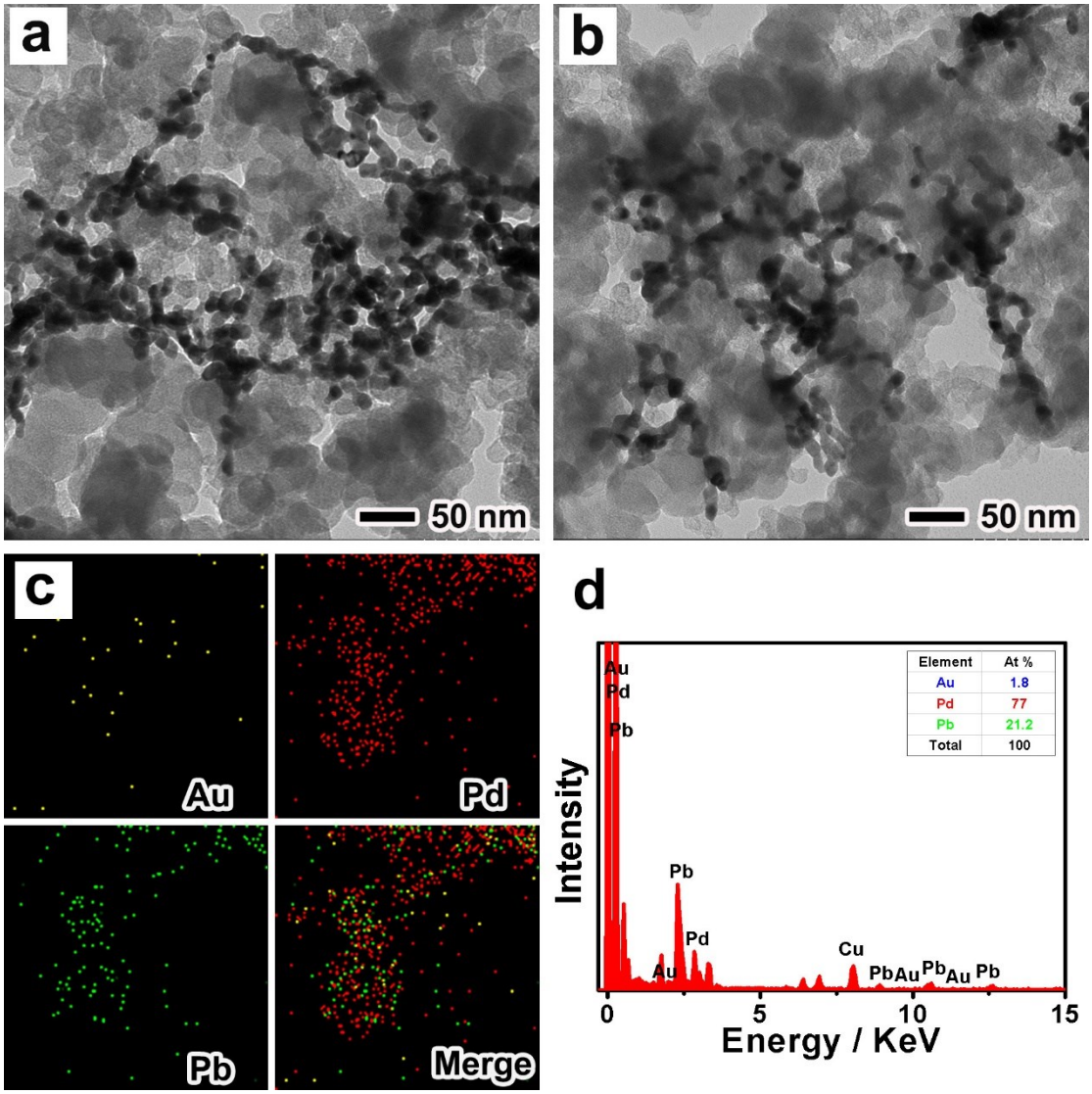

Figure S8. Representative TEM images of the 2% Au doped Pd_3Pb WNWs/C (a) before and (b) after ADT. (c) HADDF-STEM-EDX mapping image and (d) EDX spectrum of the 2% Au doped Pd_3Pb WNWs/C after 10000 cycles between 0.6 and 1.0 V versus RHE in O_2-saturated 0.1 M KOH solution.

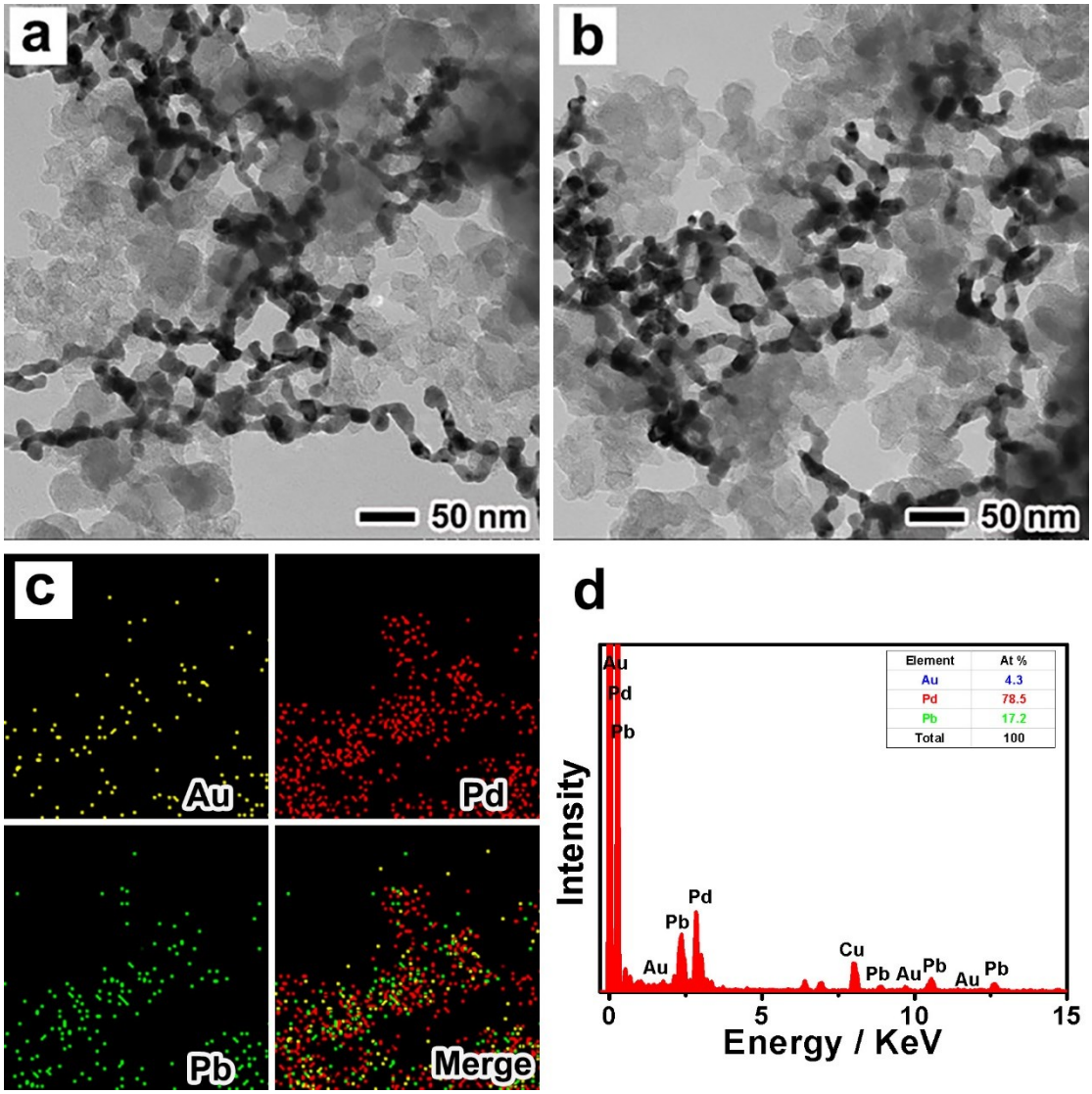

Figure S9. Representative TEM images of the 4% Au doped Pd_3Pb WNWs/C (a) before and (b) after ADT. (c) HADDF-STEM-EDX mapping image and (d) EDX spectrum of the 4% Au doped Pd_3Pb WNWs/C after 10000 cycles between 0.6 and 1.0 V versus RHE in O_2-saturated 0.1 M KOH solution.

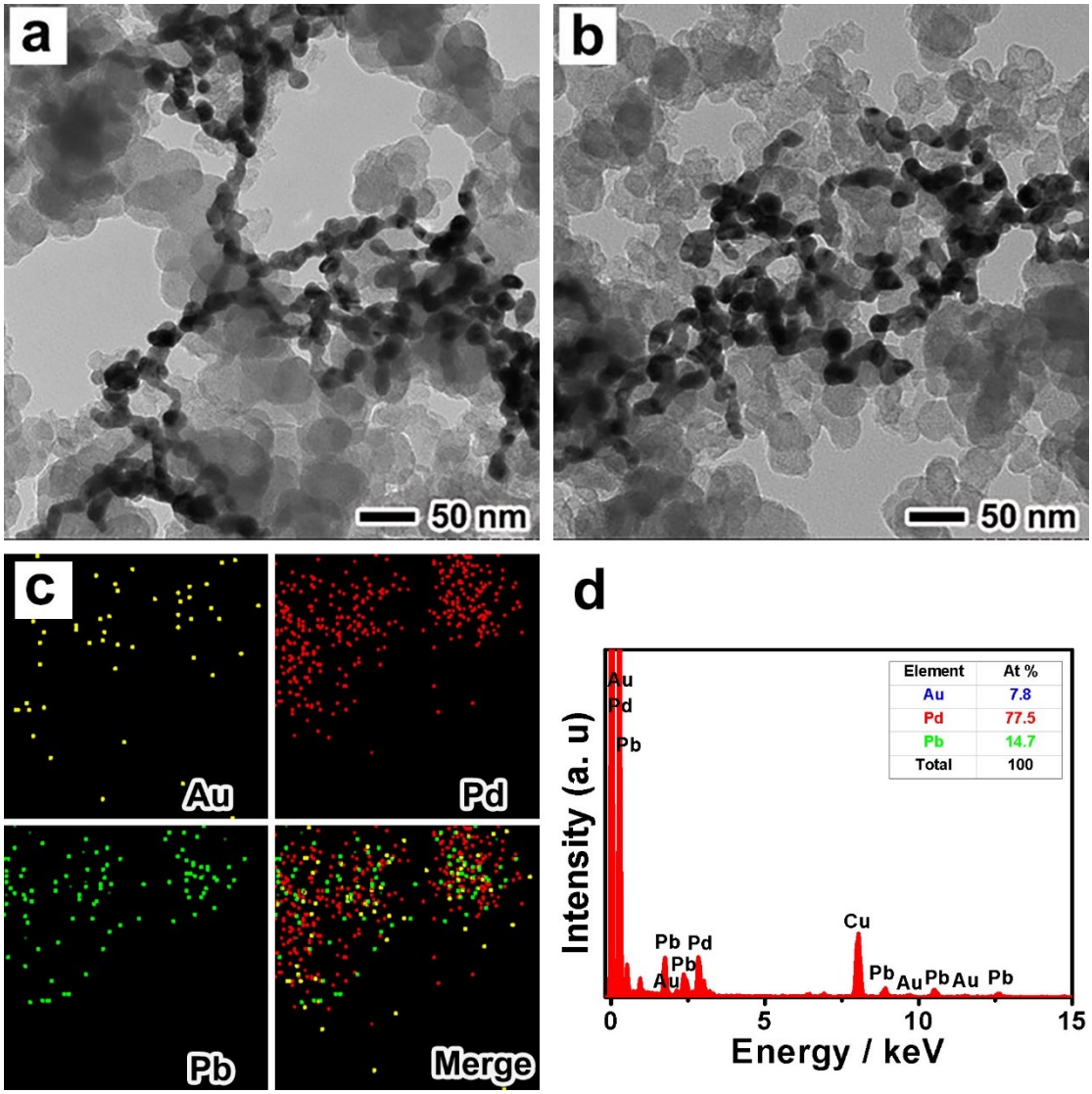

Figure S10. Representative TEM images of the 8% Au doped Pd_3Pb WNWs/C (a) before and (b) after ADT. (c) HADDF-STEM-EDX mapping image and (d) EDX spectrum of the 8% Au doped Pd_3Pb WNWs/C after 10000 cycles between 0.6 and 1.0 V versus RHE in O_2-saturated 0.1M KOH solution.

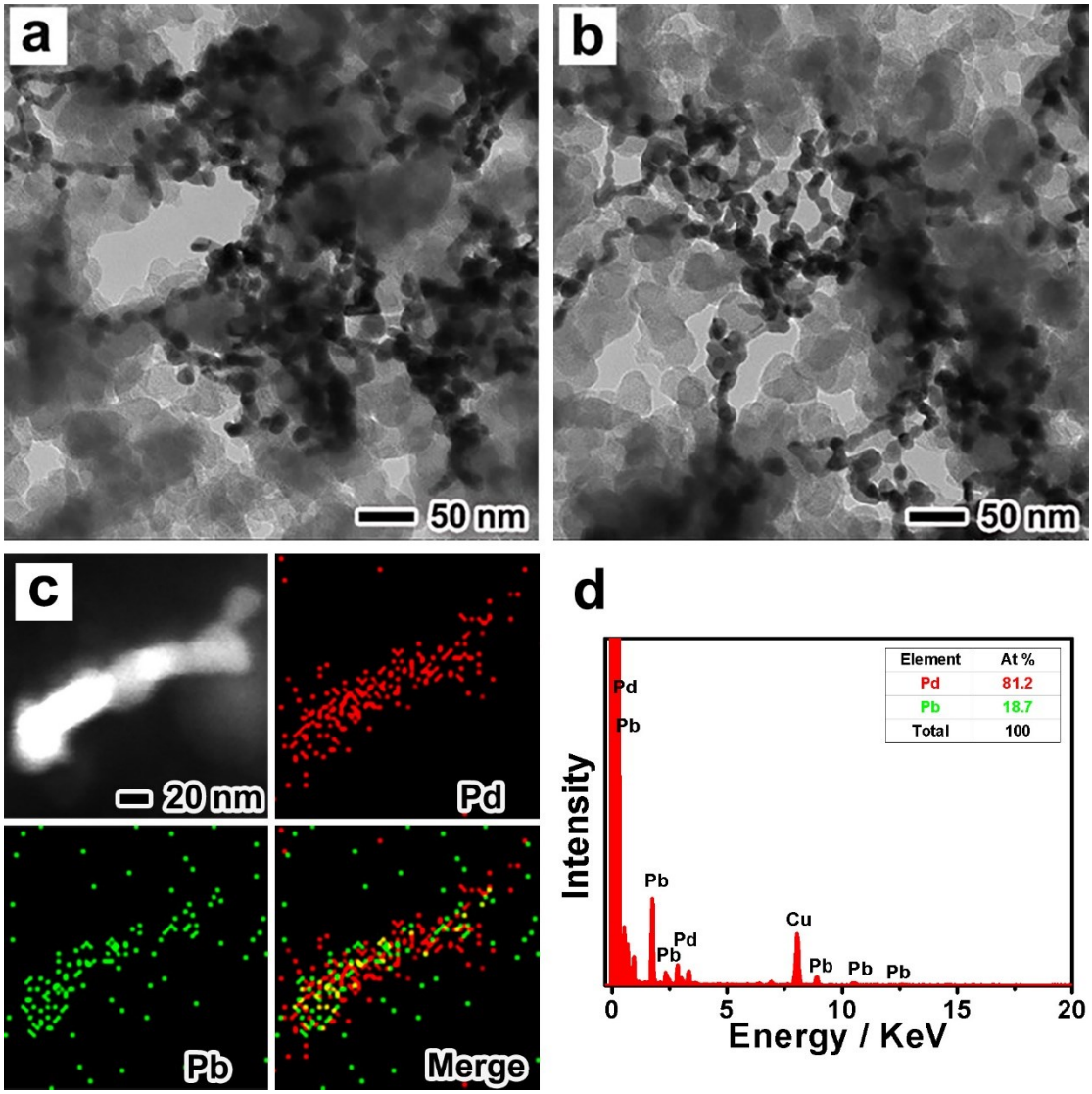

Figure S11. Representative TEM images of the Pd_3Pb WNWs/C (a) before and (b) after ADT. (c) HADDF-STEM-EDX mapping image and (d) EDX spectrum of the Pd_3Pb WNWs/C after 10000 cycles between 0.6 and 1.0 V versus RHE in O_2-saturated 0.1 M KOH solution.

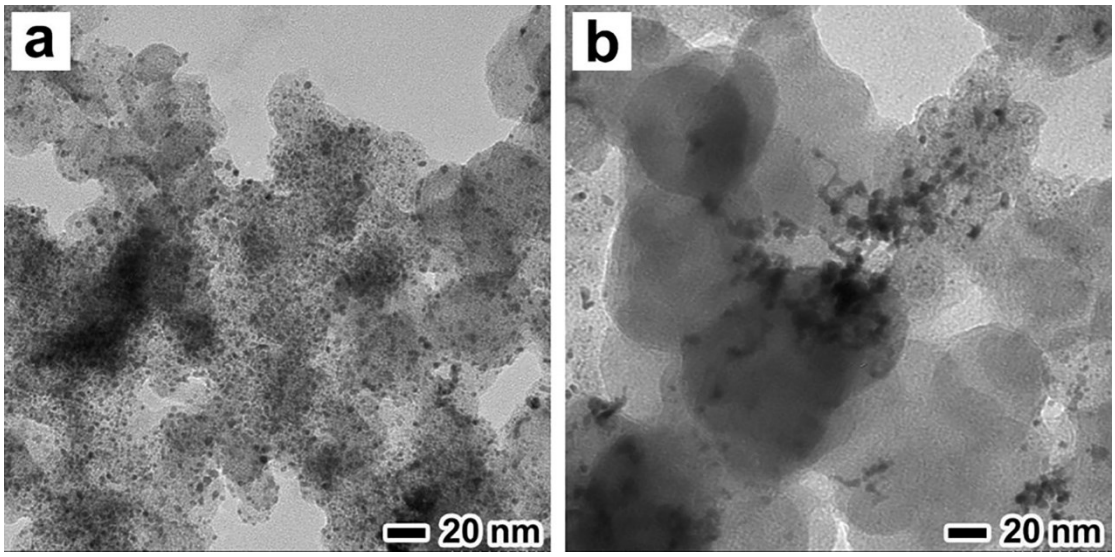

Figure S12. Representative TEM images of the commercial Pt/C (a) before and (b) after 10000 potential cycles between 0.6 and 1.0 V versus RHE in O_2-saturated 0.1 M KOH solution.

Table S1. The variations in the cell parameters of Pd_3Pb WNWs, 2% Au doped Pd_3Pb WNWs, 4% Au doped Pd_3Pb WNWs and 8% Au doped Pd_3Pb WNWs were calculated by Rietveld refinement with general structure analysis system (GSAS).

Samples	Lattice constant	χ^2	R_{wp}	R_p
Pd_3Pb WNWs	4.0376	1.19	0.0743	0.0555
2% Au doped Pd_3Pb WNWs	4.0355	1.162	0.0722	0.0559
4% Au doped Pd_3Pb WNWs	4.0272	1.489	0.0787	0.0601
8% Au doped Pd_3Pb WNWs	4.0190	1.521	0.0785	0.0602

Table S2. The ORR performance summary of the Pd_3Pb WNWs/C, 2% Au doped Pd_3Pb WNWs/C, 4% Au doped Pd_3Pb WNWs/C, 8% Au doped Pd_3Pb WNWs/C, and Pt/C including onset potential (E_{onset}), half-wave potential ($E_{1/2}$) and the kinetic current (j_k, mA/cm^2) @ 0.9 V at 1600 rpm in 0.1 M KOH solution.

No.	Samples	E_{onset} (V)	$E_{1/2}$ (V)	The kinetic current (j_k, mA/cm^2) @ 0.9 V
1	Pd_3Pb wavy nanowires/C	0.975	0.916	10.79
2	**2% Au doped Pd_3Pb wavy nanowires/C**	**0.977**	**0.919**	**13.64**
3	4% Au doped Pd_3Pb wavy nanowires/C	0.974	0.915	10.55
4	8% Au doped Pd_3Pb wavy nanowires/C	0.973	0.911	9.27
5	Pt/C	0.971	0.885	3.07

Table S3. Comparison of ORR activity of the recent reported Pd based electrocatalysts at 0.9 V vs. RHE in 0.1 M KOH. (NA: Not available)

No.	Catalysts	Mass activities ($mA/\mu g_{Pd}$)	Specific Activities (mA/cm^2)	Reference
1	**2% Au doped Pd_3Pb wavy nanowires/C**	**0.75**	**2.59**	**This work**
2	Pd@PdFe core−shell icosahedra/C	0.31	1.56	Ref. 1
3	Pd_4Sn wavy nanowires/C	0.65	1.51	Ref. 2
4	Ordered Pd_3Pb/C	0.1689	NA	Ref. 3
5	PdCuCo NPs/C-375 ^oC	0.13	NA	Ref. 4
6	The dealloyed CoAuPd/C	0.049	0.193	Ref. 5
7	PdCu tetrapods	0.29	0.73	Ref. 6
8	Pd_6Ni icosahedra	0.22	0.66	Ref. 7
9	$Ni@Pd_3$/C	0.038	0.13	Ref. 8
10	PdW alloy nanosheets flower-like superstructures/C	0.46	3.7	Ref. 9
11	PdAg nanowires/C	0.103	0.36	Ref. 10
12	Au nanowires@Pd@PEI	0.29	NA	Ref. 11
13	$PdH_{0.33}$	0.719	1.253	Ref. 12

(1) X. Li, X. Li, C. Liu, H. Huang, P. Gao, F. Ahmad, L. Luo, Y. Ye, Z. Geng, G. Wang, R. Si, C. Ma, J. Yang and J. Zeng, *Nano Lett.,* 2020, **20,** 1403-1409.

(2) Y. Zhang, B. Huang, Q. Shao, Y. Feng, L. Xiong, Y. Peng, and X. Huang, *Nano Lett.,* 2019, **19,** 6894-6903.

(3) Z. Cui, H. Chen, M. Zhao, and F. DiSalvo, *Nano Lett.,* 2016, **16,** 2560-2566.

(4) K. Jiang, P. Wang, S. Guo, X. Zhang, X. Shen, G. Lu, D. Su, and X. Huang, *Angew. Chem. Int. Ed.,* 2016, **55,** 9030-9035.

(5) L. Luo, R. Zhang, D. Chen, Q. Hu, and X. Zhou, *ACS Appl. Energy Mater.,* 2018, 1, **6,** 2619–2629.

(6) L. Zhang, S. Chen, Y. Dai, Z. Shen, M. Wei, R. Huang, H. Li, T. Zheng, Y. Zhang, S. Zhou, and J. Zeng, *ChemCatChem,* 2018, **10,** 925-930.

(7) Y. Feng, Q. Shao, Y. Ji, X. Cui, Y. Li, X. Zhu, X. Huang, *Sci. Adv.,* 2018, **4,** 8817

(8) J. Jiang, H. Gao, S. Lu, X. Zhang, C. Wang, W. Wang, and H. Yu, *J. Mater. Chem. A,* 2017, **5,** 9233-9240.

(9) X. Zhang, J. Fan, M. Han, S. Zhao, L. Lu, D. Xu, Y. Lin, N. Shi, Y. Liu, T. Lan, J. Bao, Z. Dai, *ChemCatChem,* 2020, **12,** 1-12.

(10) X. Liu, X. Yin, Y. Sun, F. Yu, X. Gao, L. Fu, Y. Wu, and Y. Chen, *Nanoscale,* 2020, **12,** 5368-5373.

(11) Q. Xue, J. Bai, C. Han, P. Chen, J. Jiang, and Y. Chen, *ACS Catal.,* 2018, **8,** 11287-11295.

(12) S. Wang, D. Tian, X. Wang, J. Qin, Y. Tang, J. Zhu, Y. Cong, H. Liu, Y. Lv, C. Qiu, Z. Gao, Y. Song, *Electrochem. Commun.,* 2019, **102,** 67-71.